Chapter 7

SNR 0101–7226: A Shell-type Supernova Remnant in the SMC with No X-ray Emission

7.1 Preface

The SMC source 0101–7226 was quite firmly identified as a supernova remnant in the 1980s based on *Einstein* X-ray data and coordinated radio and optical observations. However, subsequent work suggested that the X-ray detection is *not* associated with the SNR. The radio source is thus a potentially interesting class of SNR, and may point to the existence of other Magellanic Cloud SNR candidates having no detected X-ray emission. Although 0101–7226 was not observed as part of the survey observations reported in Chapter 4, dedicated ATCA observations were undertaken for the study reported in this chapter.

The observations and analysis reported here have been published by Taisheng Ye[1], Shaun W. Amy[1], Q. Daniel Wang[2], Lewis Ball[3] and John Dickel[4] in *Monthly Notices of the Royal Astronomical Society*, volume 275, pages 1218–1222 in 1995. The references from the original paper have been incorporated into the main bibliography and where appropriate have been updated to reflect papers that have since been published. Some minor formatting changes have been applied to maintain consistency with other chapters.

7.2 Abstract

New observations of SNR 0101–7226 in the Small Magellanic Cloud (SMC) with the Australia Telescope Compact Array and the *ROSAT* High Resolution Imager reveal a

[1]School of Physics, University of Sydney, NSW 2006, Australia.
[2]Department of Physics and Astronomy, Northwestern University, Evanston, IL 60208-3112, USA.
[3]Research Centre for Theoretical Astrophysics, University of Sydney, NSW 2006, Australia.
[4]Department of Astronomy, University of Illinois, Urbana, IL 61801, USA.

shell-type radio remnant and no significant diffuse X-ray emission. The radio images show that the remnant consists of a thick shell with a complicated filamentary structure. The low X-ray brightness, which is at least a factor of three below that of similar supernova remnants (SNRs) in the SMC, could be explained if much of the hot gas generated by the SNR has escaped into a low-density region created by a nearby OB association. Alternatively, the temperature of the hot gas downstream of the supernova shock could be relatively low, and X-ray emission could have been largely absorbed along the line of sight. We confirm the identification of a point-like X-ray source, which is spatially coincident with SNR 0101–7226, with a Be star binary system and show that the brightness of this X-ray source is variable.

7.3 Introduction

SNR 0101–7226 is an unusual supernova remnant in the Small Magellanic Cloud. It was first detected as a soft X-ray source by Seward & Mitchell (1981), using the *Einstein* Imaging Proportional Counter (IPC). Coordinated follow-up optical and radio observations were conducted. An Hα image obtained with the Anglo-Australian Telescope revealed an incomplete shell of overall dimensions $98 \times 77\,\mathrm{arcsec}^2$ with a thickness of less than 12 arcsec, centred at roughly RA $= 01^{\mathrm{h}}03^{\mathrm{m}}15^{\mathrm{s}}$, Dec. $= -72^\circ09'45''$ (J2000) (Mathewson et al. 1983a). Observations with the Molonglo Observatory Synthesis Telescope (MOST), which has an angular resolution of $45 \times 43\,\mathrm{arcsec}^2$ at this declination, showed a radio source whose centroid was well within the 2 arcmin *Einstein* error circle (Mills et al. 1982). The radio image was resolved. Although Mills et al. (1982) made no comments about the morphology of the source, the image seemed to indicate that this SNR is centrally filled. This suggests either that there is a considerable contribution to the radio emitting material in the interior of the remnant, or that the radio emission comes from a shell which is significantly thicker than that seen in Hα. Furthermore, the spectrum of the X-ray source is much harder than that of typical shell-like SNRs of similar size (Wang & Wu 1992). Recently, Hughes & Smith (1994; hereafter HS94) serendipitously detected the X-ray source in a *ROSAT* High Resolution Imager (RHRI) observation. They found that the source is point-like and argued that it is probably associated not with SNR 0101–7226, but rather with a Be star. They found no diffuse X-ray emission from SNR 0101–7226.

In this paper we present new radio and RHRI observations of SNR 0101–7226. High-resolution radio observations at 1378 and 2380 MHz were performed using the Australia Telescope Compact Array (ATCA). These data show for the first time that the SNR has a thick multi-shell morphology. The early suggestion that SNR 0101–7226 was a centre-filled remnant, and the more recent identification of the coincident point-like X-ray source with a Be star in the SMC both pointed to the possible existence of a pulsar either in or coincident with the remnant. We report the negative result of a search for a possible pulsar with the Parkes 64 m radio telescope. The results of our dedicated RHRI observation of SNR 0101–7226, which has a higher pointing accuracy than does the serendipitous observation by HS94, confirm the identification of the X-ray source

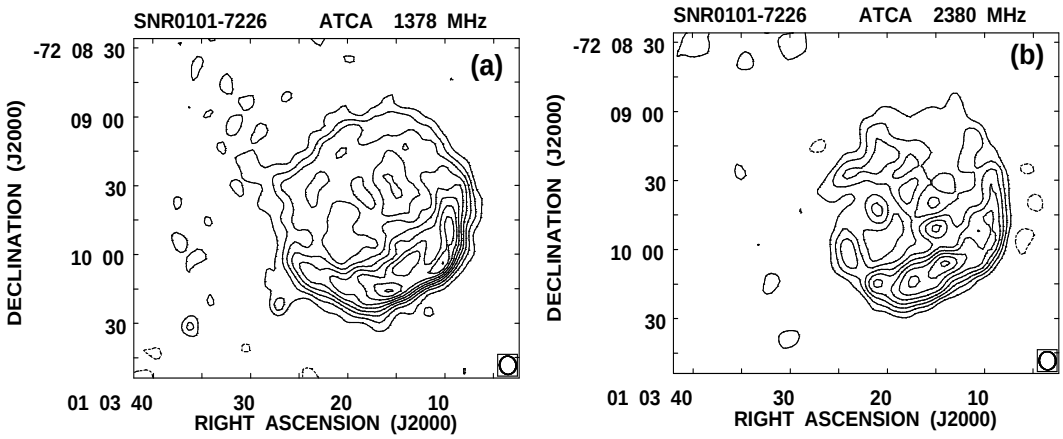

Figure 7.1: ATCA radio images of SNR 0101–7226. (a): 1378 MHz image with contour levels −0.2, 0.2, 0.4, 0.6, 0.8, 1, 1.2, 1.4, 1.6 and 1.8 mJy per beam. The resolution is ∼ 8 arcsec and the beam size (HPBW) is indicated in the bottom right hand corner. (b): 2380 MHz image with contour levels −0.15, 0.15, 0.3, 0.45, 0.6, 0.75, 0.9, 1.05 and 1.2 mJy per beam. This image has been smoothed to a resolution of ∼ 8 arcsec, and the beam size (HPBW) is indicated in the bottom right hand corner.

as the Be star binary system and provide a tighter upper limit to the diffuse X-ray emission from the SNR. These new observations further indicate that the properties of SNR 0101–7226 are strongly influenced by its environment. In particular, it is likely that the unusually low X-ray brightness of this SNR is due to the escape of hot gas, heated originally by the SNR shock wave, into a low-density region.

7.4 Observations and Results

7.4.1 The Radio Continuum

Radio continuum observations of SNR 0101–7226 were made with the ATCA on 1993 August 25 and 1994 February 10. Simultaneous observations at the central frequencies of 1378 and 2380 MHz were obtained, each consisting of 32 frequency channels spanning a bandwidth of 128 MHz. The longest and shortest baselines are 5970 and 31 m, from the 6B and 1.5B configurations respectively (Frater & Brooks 1992). Each observing run was of 12 h duration and consisted of 25 min on SNR 0101–7226 alternated with 5 min on a phase-calibrator, B0252−712. Flux density calibration was achieved by a short observation of PKS B1934−638, for which flux densities of 14.95 Jy at 1378 MHz and 11.55 Jy at 2380 MHz were assumed. The data were reduced using standard procedures for the ATCA (Killeen 1993). Deconvolution was performed using the CLEAN algorithm, and because SNR 0101–7226 was much smaller than the primary beam and was at the field centre it was not necessary to correct for the primary beam. Unfortunately, SNR 0101–7226 is too faint for the polarization to be measured with the

ATCA.

The ATCA data are presented in Figure 7.1 which shows contour maps of the radio emission at 1378 MHz (Figure 7.1a) and 2380 MHz (Figure 7.1b). The 2380 MHz map has been smoothed to the same resolution as the 1378 MHz map, namely 8 arcsec half-power-beam-width (HPBW). This serves to increase the signal-to-noise ratio at 2380 MHz and it also makes the two maps directly comparable. Both maps show a relatively thick shell of emission which is close to circular. The typical thickness of shell SNRs is $\sim$ 30 per cent of the radius (Willis 1973) while the ATCA images of SNR 0101–7226 show a shell which may be as thick as $\sim$ 40 per cent of its radius. There is considerable structure in both maps, with bright filaments in the south-west of the shell and some evidence of emission in the centre, at least in projection. The diameter of the shell in both images is $\sim$ 90 arcsec. Taking the distance to the SMC to be 57.5 kpc (van den Bergh 1989), this corresponds to a linear size of $\sim$ 25 pc.

The MOST has been upgraded considerably since it was first used to observe SNRs in the SMC (Mills et al. 1982). The telescope sensitivity has been improved and the data reduction software has become considerably more sophisticated (Turtle et al. 1998). Figure 7.2 was produced from six MOST maps of the SMC at 843 MHz, observed with different field centres and at different epochs. It has a much lower noise level than the earlier MOST image of SNR 0101–7226 published by Mills et al. (1982). In Figure 7.2, SNR 0101–7226 appears as a roughly circular source with the emission peak slightly offset from the centre toward the brightest part of the shell seen in the 1378 and 2380 MHz images shown in Figure 7.1. There is a jet-like feature emerging from the north-eastern quadrant of SNR 0101–7226. Although this feature is seen only in the lowest contour of Figure 7.2, it is visible in all individual MOST maps of SNR 0101–7226 and it also appears in the 1378 MHz ATCA map. It is therefore undoubtedly real and we return to its possible significance in Section 3.2. (A MOST image of a larger region around SNR 0101–7226 is presented by Turtle et al. 1998.)

The characteristics of the 1378 and 2380 MHz images of SNR 0101–7226, together with those of the MOST image, are given in Table 7.1. The MOST image has been calibrated by reference to the source PKS 1934−638 assuming a flux density of 13.65 Jy at 843 MHz, giving an uncertainty of $\sim$ 10 per cent. The spectral index α (where $S \propto \nu^{-\alpha}$) calculated from the integrated flux density at these three frequencies is 0.5 ± 0.2, a typical value for shell-type SNRs.

7.4.2 Pulsed Radio Emission

A search for pulsed radio emission from the direction of SNR 0101–7226 was made at 430 MHz using the 64 m Parkes radio telescope on 1993 November 20. The observation was centred at RA = $01^{\rm h}03^{\rm m}$, Dec. = $-72°09'$. The total integration time was 30 min and the sampling interval was 1.2 ms. No periodic emission was detected. The data put an upper limit of $\sim$1 mJy on the pulsed flux density at 430 MHz for a pulsar with a typical duty cycle of 5 per cent. This is consistent with a pulsar survey of the SMC by McConnell et al. (1991), at a frequency of 640 MHz and with a sensitivity of $\sim$ 1 mJy, which discovered one pulsar in the SMC but did not detect pulsations from the

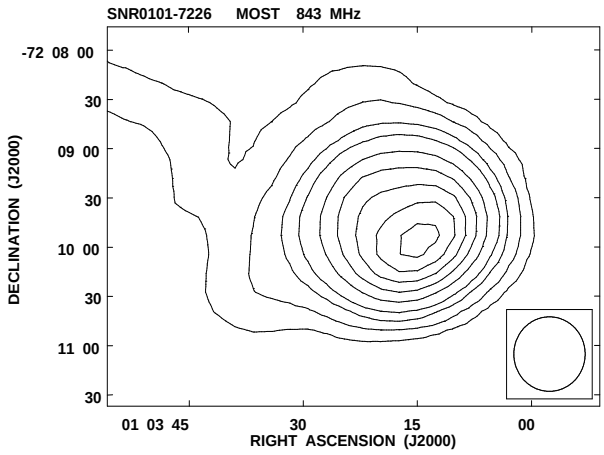

Figure 7.2: MOST radio image of SNR 0101–7226 at 843 MHz. The contour levels are 2, 4, 7, 10, 15, 20, 25, 30, 35 mJy per beam, and the beam size (HPBW) is indicated in the bottom right hand corner.

position of SNR 0101–7226.

7.4.3 X-ray Emission

The new *ROSAT* HRI observation was made between 1993 April 17 and 21, with a total usable time of 14 ks. This observation, centred on the position of SNR 0101–7226, had an on-axis 50 per cent power radius of about 3 arcsec. A systematic RHRI position error, discovered by the *ROSAT* team, was corrected by a clockwise rotation of 0.4° about the field centre (Kuerster 1993). The counts, with an original pixel size of 0.5 arcsec, were then gridded to produce an image of 1 arcsec per pixel. The observation was sensitive to photons in the energy range between 0.1 and 2 keV.

Table 7.1: Summary of the ATCA and MOST radio observations.

	ATCA		MOST
Frequency (MHz)	2380	1378	843
Resolution (arcsec)	4	8	43
Measured rms (mJy/beam)	0.07	0.1	0.6
Integrated flux density (mJy)	84	110	140

Figure 7.3 is an overlay of a contour image of the RHRI X-ray observation on a grey-scale image of the ATCA 1378 MHz radio map of SNR 0101–7226. The X-ray radiation in the region is dominated by a point-like source. The J2000 position of this point source, RA = $01^{h}03^{m}14.4^{s}$, Dec. = $-72°09'12''$ (with a 90 per cent statistical

error of ~ 1.4 arcsec), differs by 3 arcsec from that of the known Be star at RA = $01^{\rm h}03^{\rm m}13.9^{\rm s}$, Dec. = $-72^\circ09'14''$. The position difference is within the expected residual systematic error of the *ROSAT* pointing. The position of the X-ray source given by HS94, namely RA = $01^{\rm h}03^{\rm m}12.6^{\rm s}$, Dec. = $-72^\circ09'15''$, was presumably more seriously affected by systematic errors because in their observation the source was well off-axis (8.5 arcmin from the pointing centre); the rotation error alone accounts for 4 arcsec of the discrepancy. Our revised position of the *ROSAT* point source is significantly closer to the position of the Be star, and we conclude that the X-ray emission most likely comes from a binary system containing the Be star.

This conclusion is supported by the fact that the intensity of the X-ray source is variable. The count rate of the source as determined from our RHRI observation is $2.7\pm 0.6\times10^{-3}$ count s^{-1}. This is significantly lower than the value of $4.9\pm0.7\times10^{-3}$ count s^{-1} observed (with the same instrument) by HS94 in 1991 November–December. Assuming a power-law spectrum with a photon index of 1.5 and a hydrogen column density of $N_{\rm H} \sim 1.0 \times 10^{21}$ cm^{-2} (HS94), the conversion factor between the count rate and the *unabsorbed* energy flux in the 0.1−2.4 keV band is 1.3×10^{-10} (erg s^{-1} cm^{-2})/(count s^{-1}) (David et al. 1993). The corresponding source luminosity during our observation was $L_{\rm x}(0.1-2.4\,{\rm keV}) \approx 1.4 \times 10^{35}$ erg s^{-1}, while that during the observation of HS94 was $L_{\rm x}(0.1-2.4\,{\rm keV}) \approx 2.5 \times 10^{35}$ erg s^{-1}. (The latter value of $L_{\rm x}$ is higher than that quoted by HS94 – we believe the difference is that HS94 adopted a conversion factor appropriate to the *absorbed* energy flux.)

Our RHRI observation does not reveal any diffuse X-ray emission from SNR 0101–7226, a result which is consistent with the findings of HS94. By using our radio images to determine the boundary of the remnant, and exploiting the low X-ray intensity of the point source during our observation, we derive a stringent upper limit to the X-ray radiation from SNR 0101–7226. We first calculated the total observed count rate from the region within the 0.4 mJy contour of the radio emission at 1378 MHz, and then subtracted the point-source contribution and the background count rate estimated from regions outside the radio shell. The resulting 3σ upper limit to the diffuse emission is 1.8×10^{-3} count s^{-1}, which is 0.3 times the upper limit obtained by HS94. Our limit implies that the *unabsorbed* X-ray luminosity is $L_{\rm x}(0.1-2.4\,{\rm keV}) \lesssim 9 \times 10^{34}$ erg s^{-1}.

7.5 Discussion

The observations presented above raise three major points for discussion, the structure of the radio remnant as revealed by the new high-resolution observations from the ATCA, the lack of diffuse X-ray emission associated with this SNR, and the nature of the point-like X-ray source which appears within SNR 0101–7226.

7.5.1 Radio Structure

The observed radio structure of SNR 0101–7226, as shown best in Figure 7.3, could be interpreted as a thick, somewhat filamentary shell. Some of the emission situated close

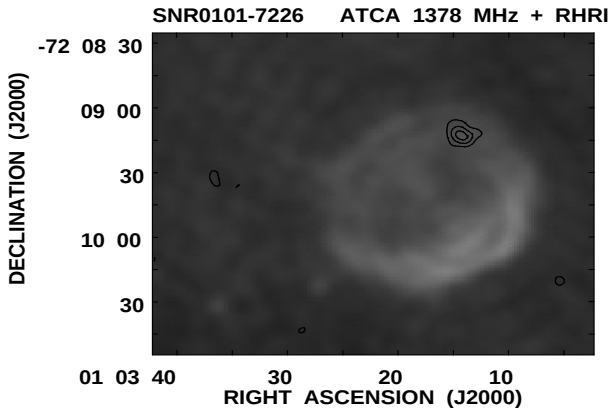

Figure 7.3: *ROSAT* HRI X-ray contour image plot superimposed on a grey-scale map of the ATCA 1378 MHz radio observations. The RHRI data have been smoothed with a Gaussian of FWHM = 4 arcsec. The contour levels are 0.030, 0.045 and 0.090 count s^{-1} $arcmin^{-2}$.

to the centre of the remnant may actually originate from the outer shell, but appear at the centre as a result of projection effects. If the central emission is of different origin from that of the outer shell, then it is likely to have a different spectrum. The radio observations at 1378 and 2380 MHz reported here have sufficient resolution, but an insufficient signal-to-noise ratio, to enable an accurate determination of the spectral index of various filaments within the remnant SNR 0101–7226. We find no evidence for variations in the spectral index across the remnant, and it is likely that all the emission originates from the outer shell.

The grey-scale image of SNR 0101–7226 shown in Figure 7.3 suggests that the radio emission has an overlapping double-ring structure. Rough eyeball fits suggest that the rings are essentially the same size, with major and minor axes measuring $\sim$ 75 and $\sim$ 90 arcsec respectively and with the same position angle of $\sim -40°$. There is also a hint that there may be two opposite cones of emission connecting the centre of the remnant to the two rings. These features are reminiscent of the bi-annular emission structures which would be found in SNRs if a bi-conical wind of relativistic particles from a central pulsar impacted on the expanding SNR shell, as suggested by Manchester (1987). Double-ring structures could then be observed when the viewing angle is close to the symmetry axis. On the other hand, it is possible that the double-ring structure apparent in Figure 7.3 is not real but is simply the result of non-uniformities in the radio emission from the outer shell of the remnant.

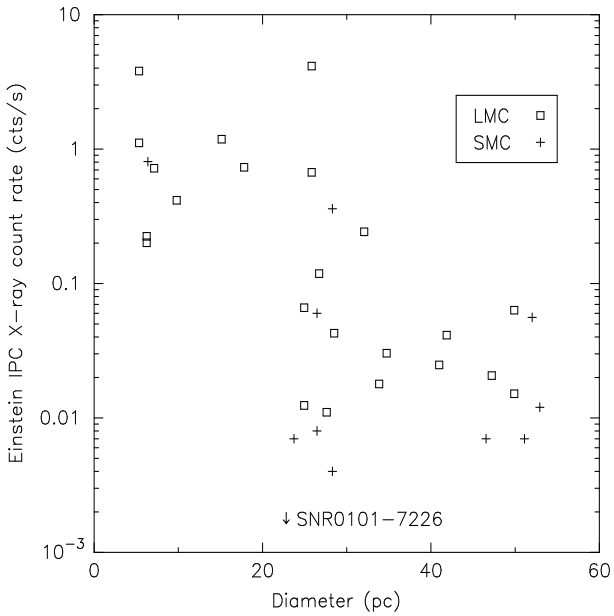

Figure 7.4: *Einstein* IPC X-ray count rate versus diameter of SNRs in the Magellanic Clouds. Both count rate and diameter have been normalized to the values appropriate for sources at the distance of the SMC (57.5 kpc). The squares and crosses indicate SNRs in the LMC and SMC respectively. The arrow indicates the 3σ upper limit on the diffuse X-ray emission from SNR 0101–7226.

7.5.2 Why No Diffuse X-ray Emission?

Figure 7.4 shows a plot of the *Einstein* Imaging Proportional Counter (IPC) X-ray count rate (Wang et al. 1991; Wang & Wu 1992 versus remnant diameter (Mills et al. 1984; Ye, Turtle & Kennicutt 1991) for SNRs in the Magellanic Clouds. Both the count rates and the diameters of the LMC remnants have been scaled as if they were at the distance of the SMC. The adopted diameters are those of the optical remnants, which in general are similar to the X-ray diameters where these are known. The RHRI and IPC instruments sample different energy ranges, $0.1 - 2.4\,\mathrm{keV}$ versus $0.16 - 3.5\,\mathrm{keV}$, and the factor relating the count rates of the two detectors from any given remnant will obviously depend on the X-ray spectrum of that remnant. However, in observations of three other SNRs in the RHRI field (Wang, in preparation) with both detectors, the RHRI count rates are only $\sim$10 per cent higher than the IPC count rates. Although there is a big scatter in Figure 7.4, particularly in the relevant diameter range of $20 - 30\,\mathrm{pc}$, it is apparent that the upper limit on the count rate of SNR 0101–7226 is at least a factor of three lower than that of all other SNRs. Therefore, the lack of diffuse X-ray emission from SNR 0101–7226 appears to be extraordinary. The low metallicity of the SMC alone could account for a delay of radiative cooling of SNRs in the SMC, compared with SNRs in the LMC, but could not explain the lack of X-ray emission from SNR 0101–7226.

We propose that the exceptionally low X-ray emissivity of SNR 0101–7226 is due

to the immediate environment into which this SNR is expanding. The high-resolution radio images of this remnant provide some clues in this regard. First, the fact that the radio shell is so much brighter in the south-western quadrant than elsewhere suggests that this part of the SNR may be bounded by a region of relatively high-density material. This is consistent with the fact that the Hα emission from this remnant is also brightest along the outer south-western part of the shell (Mathewson et al. 1983a). This raises the possibility that the high density of the material encountered by the shock has already decelerated the shock to the point where the gas temperature downstream of the shock is below the X-ray emitting temperature. Secondly, SNR 0101–7226 shows a diffuse morphology, with a thicker radio shell than many other shell-like radio SNRs. This may suggest that both magnetic field and cosmic rays are less confined in the shell, or that the pressure in the remnant is lower than is typically the case. Thirdly, the 843 MHz radio image (Figure 7.2) shows a jet-like feature emerging from the north-eastern quadrant of the remnant, and faint Hα-emitting filaments are seen outside the remnant to the east (HS94). This may indicate the outflow of energetic particles from the SNR but the low brightness of the radio feature, which is close to the sensitivity limit of our data, prevents us from investigating this possibility further. Fourthly, an Hα image of the SMC (Davies, Elliott & Meaburn 1976; hereafter DEM) shows that SNR 0101–7226 is coincident with a superbubble, DEM S 124, which includes OB associations, and many H II regions and SNRs. Together these four points suggest that SNR 0101–7226 is expanding into a region where the density gradient is large, and that diffuse hot gas generated by the SNR may have largely escaped through an opening in the north-east quadrant of the shell into the low-pressure superbubble DEM S 124. The superbubble may have been produced by the supernova explosions and stellar winds from massive stars in these OB associations. The progenitor of SNR 0101–7226 may have been a member of the OB association, denoted number 53 by Hodge (1985), which is located only a few arcminutes to the north-east of the remnant. Alternatively, the exceptionally low X-ray surface brightness of the remnant in the *ROSAT* energy range could also be explained if the X-ray absorption along the line of sight is large (e.g., $N_{\rm H} \gtrsim$ a few times $10^{21}\,{\rm cm}^{-2}$) and/or the temperature of the hot gas is relatively low (e.g., $\lesssim 0.2$ keV; David et al. 1993).

7.5.3 The Point-like X-ray Source

Our results confirm the identification of the X-ray source as an X-ray binary system containing a Be star. The ATCA radio continuum maps show no evidence of an enhancement in the radio emission at the position of the X-ray source. The 3σ upper limit is 0.3 mJy at 1378 MHz. If there is a pulsed radio signal from the compact member of the binary system, then our non-detection together with that of McConnell et al. (1991) means that it must have a flux density below $\sim$1 mJy at 430 and 640 MHz.

It is unlikely that our non-detection of radio emission from the Be star X-ray binary is simply because it was in a radio-quiet phase during our radio observations in 1993, for the following reasons. The X-ray emission was weaker in 1993 than in 1991, and weaker X-ray emission is likely to correspond to a smaller accretion rate which would

be expected to result in less scattering and dispersion of any radio emission from the source. We therefore expect an inverse relationship between the likely detectability of pulsed radio emission and the strength of the X-ray emission.

7.6 Conclusions

We have presented the results of high-resolution radio continuum and *ROSAT* HRI observations of SNR 0101–7226, together with the results of a search for pulsed radio emission coincident with this source. The non-thermal radio spectrum, the shell morphology, and the presence of a partial Hα shell leave us in no doubt that this source is indeed an SNR. However, the confirmation that previously detected X-ray emission from a position coincident with this remnant is associated with a Be star X-ray binary system, and the lack of other detectable diffuse X-ray emission from SNR 0101–7226, makes this the only known SNR in the SMC without associated X-ray emission. The radio and Hα morphologies of this remnant suggest that this lack of X-ray emission from the interior of the remnant may be explained by the escape of hot gas produced by the SNR into a low-density superbubble created by a nearby OB star association. Both the SNR 0101–7226 and the Be star could be members of the same OB association.

7.7 Acknowledgments

We thank S. Johnston and R. N. Manchester for making the Parkes pulsar observations and analysing the resulting data, and Y.-H. Chu for helpful discussions. This work has been supported by a Harry Messel Fellowship to TY, by the Lindheimer Fellowship and the NASA grant NAG5-1879 to QDW, and by NASA grant HST AR-529501-93A to JD.